Analysis of drought characteristics over Luanhe River basin using the joint deficit index

Yixuan Wang, Jianzhu Li, Ping Feng and Rong Hu

ABSTRACT

In order to describe the overall drought status objectively, a copula-based joint deficit index (*JDI*) was adopted for analyses of drought characteristics in Luanhe River basin. Monthly precipitation data from 1958 to 2011 selected from 26 rain-gauge stations were used for calculating the *JDI*. The *JDI*, which encompasses multiple deficit statuses over time scales from 1 to 12 months by using the 12-dimensional empirical copula, is shown to be capable of providing a comprehensive and objective assessment of droughts. In addition, it is demonstrated that both emerging and prolonged droughts can be captured by the *JDI*. Results of the drought evaluation over the Luanhe River basin indicate that the frequency of drought occurrence generally increases from northwest to southeast, and droughts observed in summer and autumn are more frequent and severe. Compared with the northwestern part of the area, the drought events in the southeast are characterized by longer duration and greater severity. Furthermore, a general tendency of drying is found in the flood season (July to September) over the basin, with significant aggravating trends in the southeastern part. These related drought characteristics could provide valuable information and references for regional mitigation strategies and water resource management.

Key words | copula, drought characteristics, joint deficit index, standardized precipitation index

Yixuan Wang
Jianzhu Li (corresponding author)
Ping Feng
Rong Hu
State Key Laboratory of Hydraulic Engineering Simulation and Safety,
Tianjin University,
Tianjin 300072,
China
E-mail: *lijianzhu@tju.edu.cn*

INTRODUCTION

Drought, considered as the least understood natural hazard, affects many social activities significantly and causes large economic losses (Mishra & Singh 2010; Masud *et al.* 2015). Drought commonly originates from an intense and persistent deficiency in precipitation (Zargar *et al.* 2011), but its evaluation, which is controlled by complex physical mechanisms, has different temporal and spatial characteristics (Modarres 2007; Pasho *et al.* 2011).

Up to now, a variety of drought indices (such as the Palmer drought severity index (Palmer 1965), rainfall anomaly index (Van Rooy 1965), surface water supply index (Shafer & Dezman 1982), standardized precipitation index (*SPI*) (McKee *et al.* 1993, 1995), soil moisture drought index (Hollinger *et al.* 1993), and standardized precipitation evapotranspiration index (Vicente-Serrano *et al.* 2010)), which are derived from meteorological or hydrological variables, have been established for identifying and assessing droughts. The validity and reliability of the drought index have dominant influences on the effectiveness of a drought monitoring system (Marcella & Eltahir 2008; Barua *et al.* 2010; Hosseinzadeh Talaee *et al.* 2014).

Among these drought indices, the *SPI* proposed by McKee *et al.* (1993) is the most commonly used owing to its computational simplicity and flexibility. The *SPI* measures the accumulated precipitation deficits over a given period of time in a probabilistic manner. It not only is statistically comparable across time and space, but also can represent drought conditions at various time scales (Wu *et al.* 2005; Vicente-Serrano 2006; Zarch *et al.* 2015).

Byun & Wilhite (1999) highlighted the causes of drought, which can be divided into two kinds, soil dryness and water resource deficiencies in reservoirs or other

doi: 10.2166/wcc.2015.108

sources. The amount of short-term precipitation directly affects soil moisture, and long-term precipitation totals mainly have an impact on water stored in other sources. It is thus obvious that drought is a result of the cumulative effects of water shortages over different periods of time; consequently its characteristics in terms of intensity, magnitude and duration vary with the time scale considered. For a drought assessment based on the *SPI*, a pre-specified time scale is unable to depict the entire drought condition, while inconsistent responses to different time scales will appear and cause confusion. Therefore, it is suggested that multiple *SPI*s with various time scales should be examined together to capture the overall drought status, combined with historical records and descriptions. Nevertheless, the final examined results are lacking in objectivity and probabilistic properties due to the subjective judgments involved.

On these grounds, Kao & Govindaraju (2010) proposed a joint deficit index (*JDI*) by using empirical copulas, and indicated that the *JDI* is capable of providing an objective description of the overall deficit status. Moreover, Mirabbasi *et al.* (2013) used the *JDI* for an evaluation of drought conditions in the northwest of Iran, further showing the robustness and flexibility of this index. The *JDI* serves as a probability-based drought index that can be constructed from the dependence structures of *SPI*s with time scales varying from 1 to 12 months. There seems to be a consensus that the *SPI* at a shorter time scale (1–3 months) is used for detecting meteorological or agricultural droughts, while the *SPI* on longer time scales (e.g. 6 and 12 months) well represents hydrological and water resources droughts (McKee *et al.* 1995; Vicente-Serrano & López-Moreno 2005; Mishra & Singh 2010). Hence, the *JDI*, which determines joint deficit status through the joint cumulative probability of *SPI*s, can offer an objective and overall measure of drought conditions.

The Luanhe River basin, located in north China, is of great importance for water supply to Tianjin city. Several drought-related studies have been undertaken over the basin, indicating more frequent drought events which have caused diminished water resources availability in recent decades (e.g. Li & Feng 2007; Wang *et al.* 2015a). Therefore, understanding and qualifying drought occurrence and its spatio-temporal characteristics is of particular importance for the development of adequate mitigation strategies. Although various drought indices have been used for drought monitoring and assessment in the Luanhe River basin, remarkable differences are observed in the results based on different indices (e.g. Ma *et al.* 2013; Wang *et al.* 2015b). The emergence of inconsistent results would lead to confusion in making informed decisions on a regional scale, and to some extent become an obstacle to establishing an effective monitoring and forecasting system. It is thus necessary to perform an objective assessment of the overall drought condition based on a statistical drought index, straightforwardly providing an overall concise picture of drought status in the region.

According to Kao & Govindaraju (2010), the computation of *JDI* requires only precipitation time series with a 50-year minimum recording length. Moreover the *JDI*, simply the standard normal values, are climatologically consistent for any location. As for the Luanhe River basin focused on in this study, 54-year monthly precipitation data (1958–2011) are available, and precipitation deficit is the main cause of drought in the area, accordingly showing the applicability of the *JDI* method for this area. This study aims to analyze the drought characteristics in the Luanhe River basin using the *JDI* approach, expecting to provide valuable information for water resources planners and policy makers.

STUDY AREA AND DATA

The focus of this study is on the Luanhe River basin, which is located in the northern part of the Haihe River basin, China. The basin is between 115 °30′ and 119 °15′E longitude and 39 °10′ and 42 °30′N latitude covering an area of 33,700 km^2. Its northwestern and central parts consist of mountains, while the southeast area is mainly flat. The mean annual precipitation in the basin varies from less than 400 mm in the northwest, to more than 700 mm in the southeast, and 70–80% of annual precipitation occurs from June to September. The region has a typical temperate continental monsoon climate, with a mean annual temperature of −0.3 to 11 °C. The mean annual pan evaporation over this area is 950–1,150 mm, while its mean annual actual evaporation is around 350 mm.

The Luanhe River basin was planned to provide a billion cubic meters of water per year to Tianjin city, the largest coastal city open to international trade in north China. However, due to rainfall reduction and soil and water conservation, the average annual runoff of the basin decreased by 30% after 1980 (Li & Feng 2007). Additionally, in the 21st century the consecutive droughts in the basin caused a serious insufficiency of water supplying Tianjin city, consequently aggravating environmental degradation and the water crisis. With the study area serving as an important water supply source, the occurrence and evaluation of drought there play a significant role in the social and economic development of Tianjin city.

Monthly precipitation records were collected from 26 rain-gauge stations regularly distributed throughout the Luanhe River basin (Figure 1). The precipitation series are available from January 1958 to December 2011, with a few missing values that were filled by applying linear regression (Vicente-Serrano 2006). The datasets were originally provided by the Hydrology and Water Resource Survey Bureau of Hebei Province. The location, elevation and annual average precipitation for each selected station are listed in Table 1.

METHOD

SPI and JDI

The *SPI* and the *JDI* used in this study were originally proposed by Mckee *et al.* (1993) and Kao & Govindaraju (2010), respectively.

Let $P(t)$ represent the precipitation measured at time t ($\Delta t = 1$ month in this study). For a given w-month time scale, the aggregated precipitation $X_w(t)$ with respect to t is expressed as follows:

$$X_w(t) = \sum_{i=t-w+1}^{t} P(i) \tag{1}$$

In order to reduce the degree of auto-correlation among samples and seasonal effects, 12 sub-series X_w^m were

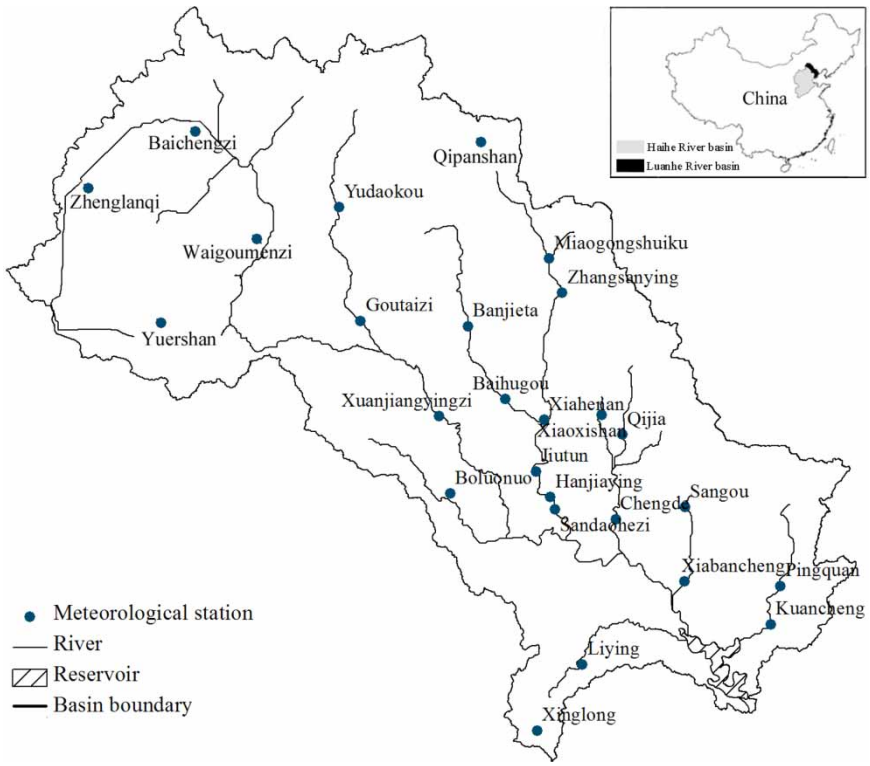

Figure 1 | Location of the Luanhe River basin and the 26 rain-gauge stations.

Table 1 | Detailed information on the 26 rain-gauge stations

Station	Location	Elevation (m)	Precipitation* (mm)	Station	Location	Elevation (m)	Precipitation* (mm)
Yuershan	116 °10′ E, 41 °41′ N	1,530	368.42	Xinglong	117 °29′ E, 40 °25′ N	620	525.46
Yudaokou	116 °58′ E, 42 °02′ N	1,400	420.33	Qijia	118 °06′ E, 41 °27′ N	610	539.02
Zhenglanqi	116 °01′ E, 42 °11′ N	1,360	355.10	Pingquan	118 °42′ E, 40 °59′ N	540	522.36
Waigoumenzi	116 °37′ E, 41 °51′ N	1,250	418.98	Bolounuo	117 °18′ E, 41 °05′ N	540	513.07
Baichengzi	116 °28′ E, 42 °17′ N	1,230	334.30	Xiahenan	117 °42′ E, 41 °18′ N	520	513.22
Banjieta	117 °30′ E, 41 °52′ N	1,070	449.48	Hanjiaying	117 °50′ E, 40 °56′ N	490	502.35
Goutaizi	117 °05′ E, 41 °33′ N	980	472.33	Xiaoxishan	117 °56′ E, 41 °11′ N	490	510.12
Qipanshan	117 °40′ E, 42 °01′ N	950	465.57	Sandaohezi	117 °42′ E, 40 °58′ N	460	517.88
Miaogongshuiku	117 °50′ E, 41 °43′ N	940	514.92	Sangou	118 °15′ E, 41 °02′ N	430	524.14
Jiutun	117 °23′ E, 41 °17′ N	850	521.06	Liying	117 °44′ E, 40 °36′ N	420	637.29
Xuanjiangyingzi	116 °52′ E, 41 °23′ N	830	502.68	Chengde	117 °56′ E, 40 °58′ N	350	512.01
Baihugou	117 °26′ E, 41 °34′ N	830	486.68	Xiabancheng	118 °10′ E, 40 °47′ N	350	546.20
Zhangsanying	117 °45′ E, 41 °34′ N	640	493.18	Kuancheng	118 °30′ E, 40 °37′ N	300	636.81

*Annual average precipitation.

obtained by dividing the series X_w based on its ending month:

$$X_w^m(g) = X_w(12(g-1)+m) \tag{2}$$

where $g = 1, 2, \ldots, n$ is the year index; $m = 1, 2, \ldots, 12$ is the month index, representing January, February, … December, respectively.

By fitting a two-parameter Gamma (G2) distribution separately for each group $x_w^m(g)$, the marginal cumulative distribution functions (CDFs) $u_w^m = F_{X_w^m}(x_w^m)$ are constructed, and then the SPI_w^m can be computed by taking the inverse normal random variables from the cumulative probability values (u_w^m):

$$SPI_w^m = \varphi^{-1}(u_w^m) = \varphi^{-1}(F_{X_w^m}(x_w^m)) \tag{3}$$

For the specified time scale of w months, the 12 subseries $SPI_w^m(g)$ were rearranged into series $SPI_w(t)$ based on time t. Drought classifications along with the corresponding SPI_w values are listed in Table 2 (Mckee *et al.* 1995). According to McKee *et al.* (1993), a drought event is defined as a period in which the SPI_w continuously reaches a value of −1.0 or less. In this study, two parameters (including drought duration and magnitude, denoted by D and M, respectively) were used to characterize the drought event. Drought duration (D) is the length of the drought period, and drought magnitude (M) is identified as follows (Mckee *et al.* 1993):

Table 2 | Drought classification of *SPI* and *JDI*

Drought condition	Index value	Drought category
Wet	Greater than 1.0	−1
Normal	−0.5 to 1.0	0
Mild drought	−1.0 to −0.5	1
Moderate drought	−1.5 to −1.0	2
Severe drought	−2.0 to −1.5	3
Extreme drought	Less than −2.0	4

$$M = -\left(\sum_{i=1}^{x} SPI_{wi}\right) \tag{4}$$

where i starts with the first month of a drought and continues to increase until the end of the drought (x) for any of the w time scale. M is commonly used for measuring the drought severity; the larger the value, the more severe the drought event.

Considering the strong seasonality of precipitation, time scales from 1, 2, to 12 months (namely $w = 1, 2, \ldots, 12$) were selected in this study. Thus, a 12-dimensional joint distribution is needed to combine the univariate marginal distributions of each time scale (u_w^m, $w = 1, \ldots, 12$). As adopted by Kao & Govindaraju (2010) and Mirabbasi *et al.* (2013), a 12-dimensional empirical copula function (Equation (5)) was employed to construct a non-parametric joint empirical probability distribution (Nelsen 2006).

$$C_n({u_1}^m, {u_2}^m, \ldots, {u_{12}}^m) = \frac{1}{n}\sum_{i=1}^{n} I\left(\frac{R_{i1}}{N+1} \le {u_{i1}}^m, \ldots, \frac{R_{i12}}{N+1} \le {u_{i12}}^m\right) \quad (5)$$

where n is the sample size; $I(A)$ denotes the indicator variable of the logical expression A, which assumes a value of 0 if A is false and 1 if A is true; $R_{i1}, \ldots, R_{i12}$ are the ranks of the ith observed data that are represented as ${u_1}^m, \ldots, {u_{12}}^m$, respectively, and u_w^m are the values of the cumulative probability of X_w^m where $w = 1, \ldots, 12$.

For the given marginal sets $\{u_1^m, \ldots, u_{12}^m\}$, the copula $C_{U_1,\ldots U_{12}}({u_1}^m, \ldots {u_{12}}^m)$ measures the cumulative joint probability $P[U_1 \ge {u_1}^m, \ldots, U_{12} \ge {u_{12}}^m] = q$ and, further, the Kendall distribution function K_c can provide the cumulative probability function $K_c(q) = P\left[C_{U_1,\ldots U_{12}}(u_1^m, \ldots u_{12}^m) \le q\right]$ (Nelsen *et al.* 2003; Nelsen 2006).

As for the 12-dimensional empirical copula, an empirical distribution function K_{Cn} can be used and is given by (Genest *et al.* 2009; Mirabbasi *et al.* 2013):

$$K_{Cn}(q) = \frac{1}{n}\sum_{i=1}^{n} I(\psi_i \le q), s \in [0, 1] \quad (6)$$

where $\psi_i = \frac{1}{n}\sum_{j=1}^{n} I({u_{1j}}^m < {u_{1i}}^m, \ldots, {u_{12j}}^m < {u_{12i}}^m)$.

The $K_c(q)$ represents the cumulative probability for events with the joint deficit status less than or equal to the given threshold q. Analogously to *SPI*, *JDI* is defined as follows:

$$JDI = \varphi^{-1}(K_C(q)) = \varphi^{-1}(P\left[C_{U_1^m,\ldots U_{12}^m}(u_1^m, \ldots u_{12}^m) \le q\right]) \quad (7)$$

Since the *JDI* is statistically similar to the *SPI*, the methods of drought classification and definition which are suitable for *SPI* can be adopted for *JDI* as well. For more details on calculating the *JDI* refer to Kao & Govindaraju (2010) and Mirabbasi *et al.* (2013).

Mann-Kendall trend test

The non-parametric Mann-Kendall (MK) trend test is one of the most widely used methods for detecting trends of hydrometeorological time series (Mann 1945; Kendall 1975). Compared with other parametric tests, this statistic method is more robust and does not assume normality of data (Lanzante 1996). In the MK trend test, the standardized test statistic Z is used as an estimator; a positive value of Z shows an increasing trend while a negative value shows a decreasing one. The Z can be calculated as follows:

$$Z = \begin{cases} (S-1)/\sqrt{\mathrm{Var}(S)} & \text{if} \quad S > 0 \\ 0 & \text{if} \quad S = 0 \\ (S+1)/\sqrt{\mathrm{Var}(S)} & \text{if} \quad S < 0 \end{cases} \quad (8)$$

$$S = \sum_{k-1}^{n-1}\sum_{j=k+1}^{n} \mathrm{sgn}(x_j - x_k), \mathrm{sgn}(x_j - x_k) = \begin{cases} +1 & \text{if} \quad (x_j - x_k) > 0 \\ 0 & \text{if} \quad (x_j - x_k) = 0 \\ -1 & \text{if} \quad (x_j - x_k) < 0 \end{cases} \quad (9)$$

where x is the variable with the observed time series ($x_1, \ldots, x_n$); n is the sample size; the test statistic S is approximately distributed normally when $n \ge 10$, with its variance $\mathrm{Var}(S) = [n(n-1)(2n+5)]/18$.

Under the null hypothesis H_0 that x are independent and randomly ordered, when $|Z| > Z_{1-\alpha/2}$, the H_0 is rejected and a significant trend exists in the time series. $Z_{1-\alpha/2}$ is the critical value of Z from the standard normal table, and for 10% significance level the value of $Z_{1-\alpha/2}$ is 1.28.

RESULTS AND DISCUSSION

SPI and JDI

The 1- to 12-month cumulative precipitation series for each month and each station are fitted with a two-parameter Gamma (G2) distribution, using the maximum likelihood (ML) method to estimate parameters of the distribution.

The Kolmogorov–Smirnov (KS) test was then applied for the goodness of fit at the 1% significance level. Results show that more than 95% of the cases passed the KS tests, indicating that the G2 distribution is an appropriate distribution for constructing the *SPI* and *JDI* in the Luanhe River basin.

Figure 2 illustrates the evolution of 1- and 12-month *SPI* and *JDI* during the period 1959–2011 at Chengde station. The SPI_1 series with greater fluctuation indicate that the droughts identified at a shorter time scale have higher temporal frequency and shorter durations, while the *SPI* with a longer time scale (SPI_{12}), varying more smoothly, captures the drought events that are less frequent but lasted longer. As a whole, the *JDI* series show a similar temporal behavior to the SPI_{12}. Nevertheless, when marked differences exist in the multiple *SPI*s, the *JDI* appears to give a better explanation for the drought condition. For example, the period of February 2010 to June 2010, with sufficient precipitation, is assigned to a wet episode according to the SPI_1. However, due to the serious water deficit accumulated in earlier months, this period is dominated by moderate drought conditions, evident in the SPI_{12}. The *JDI*, which is capable of capturing the joint behaviors of *SPI*s over various time scales, defines the overall deficit status in this period as normal.

According to historical records and related literature, drought events mainly occurred in 1961, 1963, 1968, 1972, 1980–1984, 1997–2007 and 2009 for the study area. Based on the series of SPI_3, SPI_6, SPI_{12} and *JDI*, the parameters (including drought duration (*D*) and magnitude (*M*)) of the above drought events are reported in Table 3, taking Chengde station as an example.

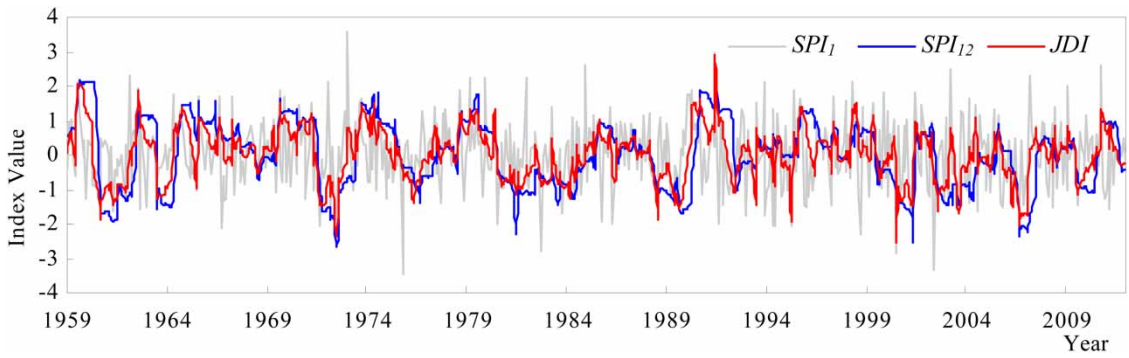

Figure 2 | SPI_1, SPI_{12} and *JDI* series at Chengde station.

Table 3 | Comparison of drought characteristics based on different indices values

	Historical record			SPI_3		SPI_6		SPI_{12}		*JDI*	
Main drought event	**Beginning date**	**D**	**Drought condition**	**D**	**M**	**D**	**M**	**D**	**M**	**D**	**M**
1961	Apr 1961	9	Extreme drought	3	4.03	6	7.12	20	30.32	8	11.45
1963	Jul 1963	5	Severe drought	2	2.89	6	8.07	11	15.08	6	9.11
1968	Jul 1968	2	Mild drought	2	2.55	\	\	\	\	2	2.67
1972	Apr 1972	6	Extreme drought	3	4.76	5	4.42	14	22.7	6	11.35
1980–1984	Feb 1981	8	Severe drought	1	1.03	4	4.24	10	10.96	7	8.82
	Mar 1984	3	Moderate drought	1	1.17	2	3.57	3	3.44	2	3.48
1997–2007	Jul 2000	8	Extreme drought	3	5.43	6	10	12	19.63	8	14.9
	Jul 2002	6	Severe drought	3	4.38	6	8.27	10	13.19	5	7.86
	Jul 2006	6	Moderate drought	5	7.7	8	14.46	11	21.23	8	12.9
2009	Aug 2009	\	Severe drought	1	1.4	4	4.45	9	9.58	5	5.78

Note: unit of drought duration (*D*) is one month.

It can be seen in Table 3 that both *SPI* and *JDI* have the ability to identify and assess the historical drought events, but values of the drought parameters defined by these indices are different from each other. Short-term *SPI* values are more sensitive to emerging droughts, while a long-term *SPI* value shows a strong response to a prolonged drought. For example, the mild drought starting in July 1968 cannot be captured by the long-term *SPI* (namely SPI_6 and SPI_{12}), while the SPI_3 indicates this drought event with a duration of 2 months, which is also suggested by the *JDI*. In the case of the extreme drought that occurred in 2000, the drought parameters obtained by the multiple *SPI*s have great differences (e.g. the *D* and *M* of SPI_{12} are four times larger than the corresponding ones of SPI_3), but a duration of 8 months defined by the *JDI* is consistent with the historical record. Among the multiple *SPI*s, the SPI_6 shows better performance in capturing historical drought events in the study area, since the general agreement of its assessment results and historical records seems good. However, when considering the short-term drought in 1968 and the extreme droughts in 1961 and 1972, remarkable differences are exhibited especially in terms of drought magnitude. Compared with the SPI_6, the results of *JDI* are in better agreement with historical records for all the cases listed in Table 3 on the whole. For instance, the extreme drought event that occurred in 1972 lasted 6 months, affecting an area of 30,000 km^2 in Chengde city. It was reported to be the most severe drought event since 1919 and caused great damage to the eco-environment and socio-economy in this region (Gao 1998). According to the *JDI*, the corresponding assessment result with a duration of 6 months and a magnitude of 11.35 replicates this drought condition well. It is indicated that the *JDI*, which integrates the deficit status over various durations (from 1 to 12 months), can avoid the confusion caused by multiple *SPI*s with different time scales, and accurately define and assess overall drought conditions.

Four cases with the drought categories based on SPI_w ($w = 1, 2, \ldots, 12$) and *JDI*, as well as the corresponding 1- to 12-month precipitation, were selected and presented in Figure 3.

As shown in Figure 3(a), values of *SPI* at all time scales for June 1972 indicate severe and even extreme drought conditions due to serious precipitation deficits. The *JDI* that represents the joint deficit status also suggests an extreme drought for this case. In the case of July 1972 (Figure 3(b)), the SPI_1 assigned to a wet class shows sufficient precipitation in this month, while the *SPI*s with other time scales reflect a drought state due to precipitation deficits in prior months. The *JDI* takes the effect of preceding serious deficits into account, and reports a severe drought in this instance.

For December 1993 (Figure 3(c)), SPI_1 reports a severe drought since hardly any precipitation was observed. However, other *SPI*s with longer memory cannot capture an emerging drought in a timely manner, showing above normal conditions. The *JDI* indicates a mild drought condition for this instance, demonstrating that the *JDI* not only can reflect the emerging drought but also has temporal memory for accumulated deficit. Figure 3(d) shows a confusing case in April 2007, in which *SPI* with time scales from 1 to 5 months show approximately normal precipitation in the last five months, while other *SPI*s accounting for the preceding serious deficit report drought status with different severity. Based on the entire dependence structure of multiple *SPI*s, the *JDI* reflects a mild drought condition in this case.

Figure 4 shows regional illustrations of the drought condition for December 2000 based on SPI_1, SPI_3, SPI_6, SPI_9, SPI_{12} and *JDI*. According to historical records, the Luanhe River basin suffered widespread drought in 2000, with most areas experiencing severe to extreme droughts especially for the period June to September. Compared with the southeast area, the drought condition in the northwest was more serious and longer lasting. In October and November 2000, sufficient precipitation was observed and hence the short-term preceding deficit seemed to be relieved to some extent. Therefore, for December 2000, the 1- and 3-month *SPI* indicate that the deficit status has come back to normal overall (Figure 4(a) and 4(b)). At the time scale of 6 and 9 months the drought condition was in its development stage, and SPI_6 and SPI_9 show more severe precipitation deficits in the southeast (Figure 4(c) and 4(d)). The *SPI* at the 12-month time scale is expected to involve the accumulated water deficit during the entire duration of drought and determines drought status in most sites (Figure 4(e)), but its longer memory delays the response for the increased precipitation in recent months (October and November). The JDI, which reports normal status in

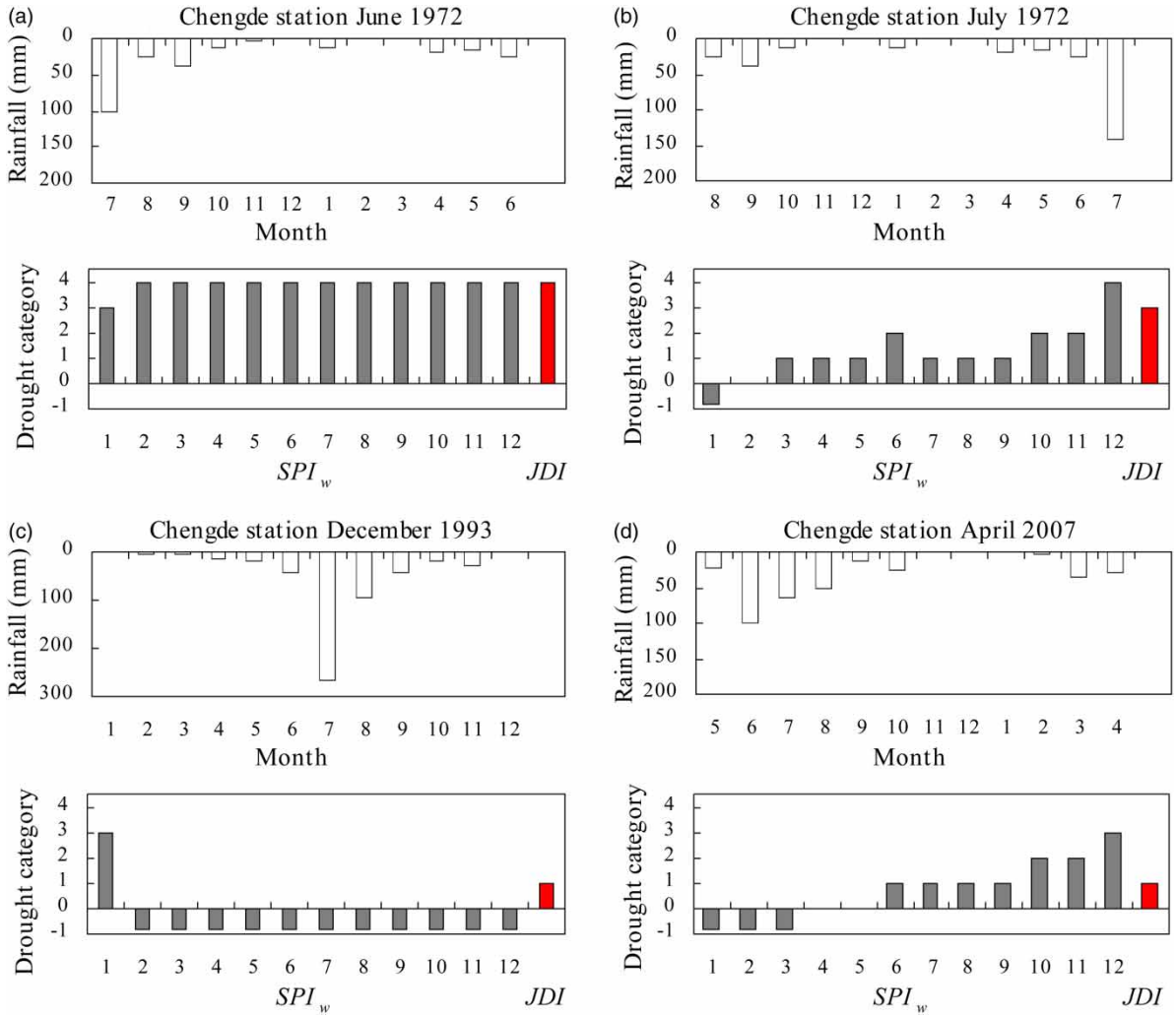

Figure 3 | Results of drought assessment based on *SPI* and *JDI* and the corresponding precipitation for four selected cases.

most areas but determines mild to moderate droughts in the central part (Figure 4 (f)), not only reflects the effect of precipitation supply in a timely manner, but also effectively considers the temporal memory for moisture deficit. These results support the conclusion that the *JDI* is capable of capturing both emerging and prolonged droughts in a timely manner, which is demonstrated by Kao & Govindaraju (2010).

Drought characteristics based on *JDI*

The frequency of drought occurrences for each drought category was calculated using *JDI*, considering the periods of 1959–1969, 1970–1979, 1980–1989, 1990–1999 and 2000–2011, and four seasons (namely, spring (March to May), summer (June to August), autumn (September to November) and winter (December to February)). As an average of the 26 stations, the frequency associated with the mild, moderate, severe and extreme drought expressed as percentages are given in Figures 5 and 6 for different periods and different seasons, respectively.

Figure 5 shows that the frequencies related to severe and extreme drought classes generally tend to increase over time, especially in the most recent decade, which is consistent with previous studies (Li & Feng 2007; Wang *et al.* 2015a). In Figure 6, it can be seen that mild droughts observed during 1959–2011 mostly occurred in the autumn. The maximum frequencies associated with

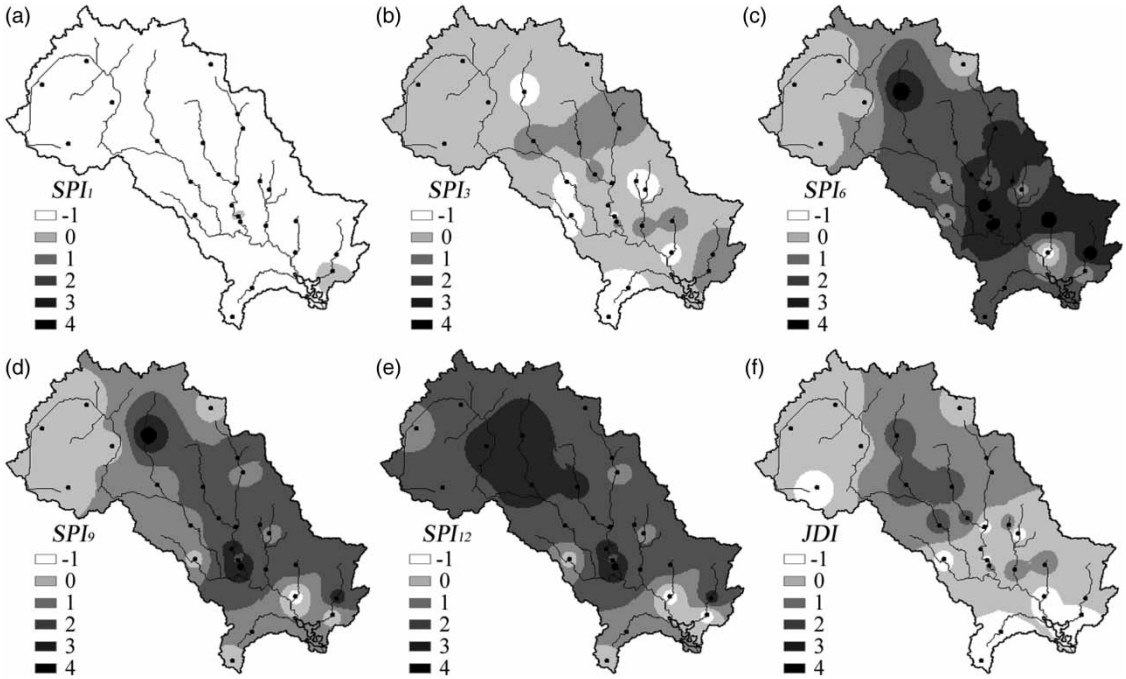

Figure 4 | Regional illustration of the drought condition of the study area for December 2000.

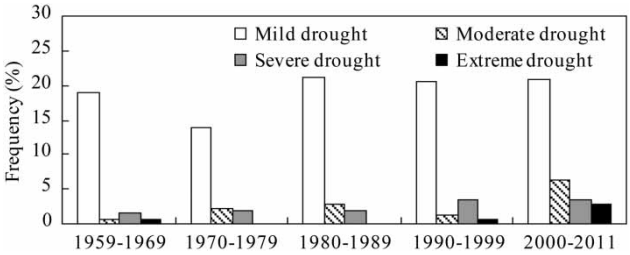

Figure 5 | Frequencies of drought in different years.

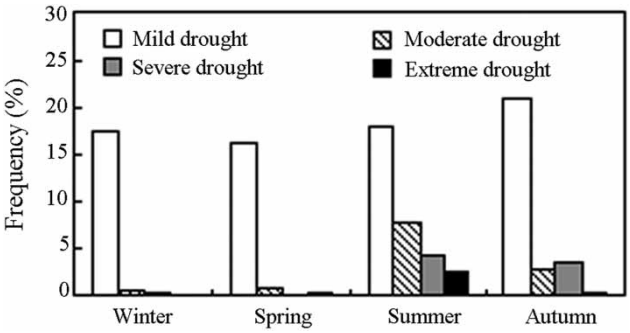

Figure 6 | Frequencies of drought for different seasons.

moderate, severe and extreme drought occur in summer, indicating that summer droughts seem to be more frequent and severe.

In the Luanhe River basin, the precipitation in summer and autumn (from June to November) accounts for more than 80% of annual precipitation, predominating in the water budgets of the hydrological cycle. Most of the regional agricultural production is from irrigated agriculture, and the corresponding agricultural activities are concentrated in summer and autumn. Moreover, sufficient precipitation during the flood season (from June to September) serves as a key element for an adequate reservoir storage which directly guarantees the quality of water supply for Tianjin city. Consequently, the severe and frequent droughts in summer and autumn have seriously affected river ecosystems and irrigated agriculture in the basin, resulting in crop failures, water scarcity and environmental degeneration. In the most recent decade, Tianjin city has faced a water crisis due to the inadequate supply of water, as a response to the frequent occurrence of extreme droughts in the Luanhe River basin. It is thus of great significance for the Luanhe River basin to improve drought mitigation strategies and water resources management.

In this study, the non-parametric MK trend test was used to detect the trend of the *JDI* series during 1959–2011, and the Z statistics of the MK test for each month and each station are listed in Table 4. Based on the Z statistics of the MK test, a

Table 4 | Z Statistics of MK trend test based on *JDI* for each month and station in the study area

Station	Jan	Feb	Mar	Apr	May	Jun	Jul	Aug	Sep	Oct	Nov	Dec
Yuershan	0.38	0.84	0.75	0.77	0.91	0.86	−0.44	−1.01	−0.92	−0.76	0.45	0.62
Zhenglanqi	0.43	0.59	0.51	0.50	0.83	0.53	−0.27	−1.54*	−1.37*	−0.51	0.39	1.02
Baichengzi	0.37	0.45	0.41	0.43	0.75	0.68	−0.57	−1.16	−1.91*	−0.33	0.45	0.75
Waigoumenzi	0.85	0.92	0.58	0.89	1.03	0.96	−0.39	−0.89	−1.07	−0.81	0.78	1.62*
Yudaokou	0.44	0.94	0.71	0.62	1.70*	1.04	−0.37	−1.56*	−1.07	−0.61	0.38	1.62*
Goutaizi	1.21	0.87	0.37	0.33	1.23	−0.12	−0.35	−1.48*	−0.86	−0.30	−0.61	0.04
Jiutun	−1.49*	−2.06*	−2.52*	0.18	0.64	0.35	−1.05	−0.84	−1.42*	−0.93	−0.85	−0.91
Xuanjiangyingzi	−2.50*	−1.66*	−2.19*	−0.38	0.29	0.32	−0.23	−2.88*	−1.34*	0.08	−0.87	−1.17
Sandaohezi	−1.79*	−1.50*	−1.89*	0.11	0.90	−1.65*	−0.75	−1.93*	−1.68*	−1.14	−0.20	−1.17
Qipanshan	0.56	0.48	0.59	0.62	0.87	0.75	−0.63	−1.39*	−0.75	−0.89	0.45	1.36*
Miaogongshuiku	0.95	−0.08	0.31	1.51*	1.33*	1.20	0.54	−1.01	−0.51	−0.31	0.19	0.91
Zhangsanying	0.67	0.11	0.79	1.25	1.51*	0.32	0.64	−0.45	−0.46	0.00	−0.25	−0.02
Banjieta	0.70	0.79	0.55	−0.61	0.95	0.39	−0.83	−1.20	−0.65	0.27	−0.23	−1.79*
Baihugou	0.68	0.75	−1.14	0.28	0.94	−0.04	−0.43	−0.87	−1.18	−0.22	−0.03	−0.89
Xiahenan	−0.59	−0.89	−1.19	1.12	2.00*	0.89	−0.93	−0.91	−1.55*	−0.61	0.15	−1.06
Hanjiaying	−0.28	−0.69	−1.15	0.60	0.85	0.77	−0.94	−1.55*	−0.93	−0.36	0.20	−0.42
Qijia	−1.02	−0.45	−0.69	0.04	1.93*	1.66*	0.01	−0.94	−0.85	0.71	0.96	0.74
Xiaoxishan	−1.54*	−0.36	−1.29*	0.38	1.68*	1.17	−0.35	−0.92	−0.75	−0.55	−0.07	−1.17
Chengde	−0.64	−0.77	−1.94*	−0.55	−0.51	−1.82*	−1.12	−1.49*	−1.07	0.11	−0.09	0.22
Sangou	−1.53*	−1.60*	−2.15*	−0.47	1.01	0.69	−0.22	−2.08*	−1.31*	−0.45	−1.33*	−1.96*
Xinglong	−1.48*	−1.56*	−1.50*	−0.30	0.26	0.35	−1.05	−1.36*	−1.34*	−0.57	−0.38	−1.10
Liying	−0.84	−0.82	−1.25	−0.41	0.81	1.39*	−0.31	−1.48*	−0.94	−0.35	0.11	−0.36
Pingquan	−0.44	−1.63*	−1.43*	−0.71	0.05	0.37	−0.05	−1.38*	−1.05	−0.41	−0.73	−0.32
Kuancheng	−1.89*	−1.96*	−1.74*	−0.97	1.25	1.17	−1.03	−1.50*	−1.04	−1.09	−1.82*	−1.04
Bolounuo	−1.47*	−1.44*	−2.63*	−0.67	0.11	0.39	−1.12	−1.66*	−2.04*	−1.02	−1.14	−0.83
Xiabancheng	−2.28*	−1.79*	−1.54*	−0.91	0.80	−1.91*	−1.60*	−2.39*	−1.30*	−0.64	−0.84	−1.30*

*Significant trend at the 90% confidence level.

positive value shows a mitigating trend of drought condition, while a negative value shows an aggravating trend. In August and September, negative Z values are observed in all the stations, and show significance at the 90% confidence level for the stations located in the southeast. It is indicated that the drought in August and September has an aggravating trend over the basin, shown to be significant in the southeastern part. Z values for July are found to be negative in about 85% of the selected stations, suggesting aggravating trends of drought condition in July. Moreover, more than 50% of the stations show significant aggravating trends in January, February and March droughts, and these stations are mostly located in the southeast. For the drought condition in May and June, positive Z values were found in more than 75% of the stations, reflecting mitigating trends.

The spatial distributions of drought frequency, mean drought duration and mean drought magnitude over the period of 1959–2011 are presented in Figure 7. The drought frequency within the basin varies from 38.5% (Liying station located in the south) to 12.7% (Miaogongshuiku station located in the north), showing a highly uneven spatial distribution (Figure 7(a)). In general, the frequency of drought occurrence is increasing from the northwest to the southeast in the study area. As for the mean drought duration and mean drought magnitude (Figure 7(b) and 7(c)), the higher values are observed in the stations which are mainly located in the southeastern part, while the stations with the lower values are located in the northwest, which corresponds to the results of the MK test. The Bolounuo station, with the longest mean duration (6.1 months) and maximum mean magnitude (14.34), lies at the south of the basin. The Yudaokou station in the northwest has the shortest mean duration (2.7 months) and minimum mean magnitude (4.11).

CONCLUSIONS

In this paper, monthly precipitation data from 26 rain-gauge stations over the period of 1958 to 2011 were selected to calculate the *JDI*. The *JDI* series were then employed to analyze the drought characteristics in the basin. The main conclusions are summarized as follows.

As a probability-based drought index, the *JDI* takes the effects of water deficits at various time scales into account, objectively reflecting the overall drought status. Compared with the *SPI*, the *JDI* can not only provide a more comprehensive drought assessment, but also characterize drought conditions more accurately. Moreover, the *JDI* constructed in terms of the joint cumulative probability is able to capture both emerging and prolonged droughts effectively, and is shown to be a flexible and appropriate tool for drought monitoring and assessment.

During the period of 1959–2011, serious drought events mainly occurred in summer and autumn in the Luanhe River basin, and extreme droughts appeared frequently in the most recent decade, seriously hitting the river ecosystems, irrigated agriculture and water supply capacity of the basin. Compared with the northwest in the basin, more severe and frequent droughts are observed in the southeast. In addition, the drought condition over the basin tends to be aggravating in August and September, with significant

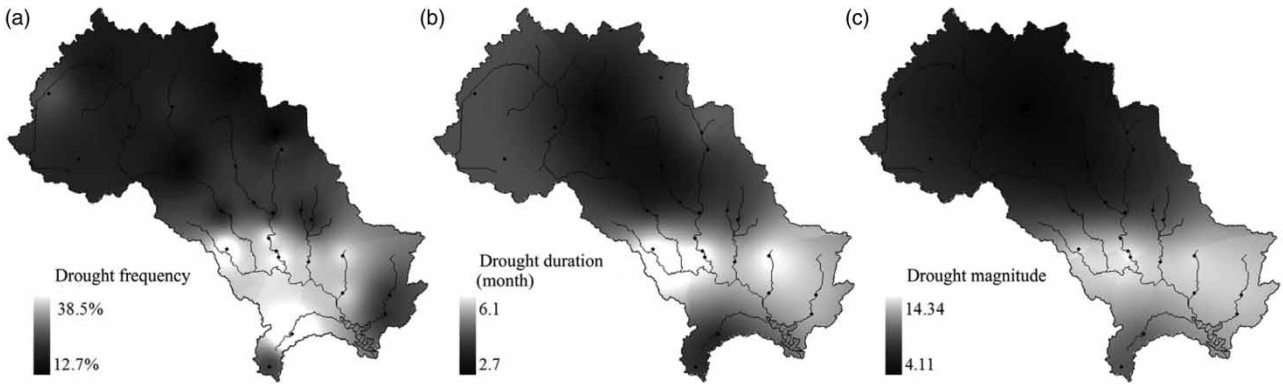

Figure 7 | Regional illustration of drought frequency, mean drought duration and mean drought magnitude over the period of 1959–2011 in the Luanhe River basin.

aggravating trends in the southeast. The occurrence and evaluation of droughts can be objectively described by the *JDI*, providing valuable information and references for developing regional mitigation strategies and water resources management.

The *JDI* constructed in this study is purely dependent on precipitation deficits over the time scales of 1 month to 12 months. However, under a drought condition, multiple moisture deficits could be observed in many other hydrologic variables (such as streamflow, soil moisture and reservoir storage), which are also varying with the time and spatial scales considered. Therefore, future studies should detect the dependence structures of these different types of deficits in a systematic manner, so as to construct an inter-variable drought index that is more representative for the joint behavior of regional droughts. Moreover, the drought forecast and risk assessment performed based on the *JDI* should be the subject of further study.

ACKNOWLEDGEMENTS

This work was financially supported by the National Natural Science Foundation of China (No. 51479130). The authors thank the Hydrology and Water Resource Survey Bureau of Hebei Province for providing the observed precipitation data.

REFERENCES

Barua, S., Perera, B. J. C., Ng, A. W. M. & Tran, D. 2010 Drought forecasting using an aggregated drought index and artificial neural network. *Journal of Water and Climate Change* **1** (3), 193–206.

Byun, H. R. & Wilhite, D. A. 1999 Objective quantification of drought severity and duration. *Journal of Climate* **12** (9), 2747–2756.

Gao, J. H. 1998 Elementary research of the tendency in Chengde's environment development in the past 300 years. *Arid Zone Research* **15** (2), 70–74 (in Chinese).

Genest, C., Rémillard, B. & Beaudoin, D. 2009 Goodness-of-fit tests for copulas: a review and a power study. *Insurance: Mathematics and Economics* **44**, 199–213.

Hollinger, S. E., Isard, S. A. & Welford, M. R. 1993 A new soil moisture drought index for predicting crop yields. In: *8th Conference on Applied Climatology, Anaheim, CA*. American Meteorological Society, pp. 187–190.

Hosseinzadeh Talaee, P., Tabari, H. & Sobhan Ardakani, S. 2014 Hydrological drought in the west of Iran and possible association with large-scale atmospheric circulation patterns. *Hydrological Processes* **28** (3), 764–773.

Kao, S. C. & Govindaraju, R. S. 2010 A copula-based joint deficit index for droughts. *Journal of Hydrology* **380** (1), 121–134.

Kendall, M. G. 1975 *Rank Correlation Methods*. 4th edn. Charles Griffin, London.

Lanzante, J. R. 1996 Resistant, robust and non-parametric techniques for the analysis of climate data: theory and examples, including applications to historical radiosonde station data. *International Journal of Climatology* **16**, 1197–1226.

Li, J. Z. & Feng, P. 2007 Runoff variations in the Luanhe river basin during 1956–2002. *Journal of Geographical Sciences* **17** (3), 339–350.

Ma, H. J., Yan, D. H., Weng, B. S., Fang, H. Y. & & Shi, X. L. 2013 Applicability of typical drought indexes in the Luanhe River Basin. *Arid Zone Research* **30** (4), 728–734 (in Chinese).

Mann, H. B. 1945 Nonparametric tests against trend. *Econometrica* **13**, 245–259.

Marcella, M. P. & Eltahir, E. A. B. 2008 The hydroclimatology of Kuwait: explaining the variability of rainfall at seasonal and interannual time scales. *Journal of Hydrometeorology* **9** (5), 1095–1105.

Masud, M. B., Khaliq, M. N. & Wheater, H. S. 2015 Analysis of meteorological droughts for the Saskatchewan River Basin using univariate and bivariate approaches. *Journal of Hydrology* **522**, 452–466.

McKee, T. B., Doesken, N. J. & Kleist, J. 1993 The relationship of drought frequency and duration to time scales. In: *Proceedings of the 8th Conference on Applied Climatology*. American Meteorological Society, Boston, pp. 179–184.

McKee, T. B., Doesken, N. J. & Kleist, J. 1995 Drought monitoring with multiple time scales. In: *Proceedings of the 9th Conference on Applied Climatology*. American Meteorological Society, Boston, pp. 233–236.

Mirabbasi, R., Anagnostou, E. N., Fakheri-Fard, A., Dinpashoh, Y. & Eslamian, S. 2013 Analysis of meteorological drought in northwest Iran using the joint deficit index. *Journal of Hydrology* **492**, 35–48.

Mishra, A. K. & Singh, V. P. 2010 A review of drought concepts review article. *Journal of Hydrology (Amsterdam)* **391** (1–2), 202–216.

Modarres, R. 2007 Streamflow drought time series forecasting. *Stochastic Environmental Research and Risk Assessment* **21** (3), 223–233.

Nelsen, R. B. 2006 *An Introduction to Copulas*. Springer, New York.

Nelsen, R. B., Quesada-Molina, J. J., Rodríguez-Lallena, J. A. & Úbeda-Flores, M. 2003 Kendall distribution functions. *Statistics & Probability Letters* **65**, 263–268.

Palmer, W. C. 1965 *Meteorological Drought*. US Weather Bureau Tech Paper 45, pp. 1–58.

Pasho, E., Camarero, J. J., de Luis, M. & Vicente-Serrano, S. M. 2011 Impacts of drought at different time scales on forest growth across a wide climatic gradient in north-eastern Spain. *Agricultural and Forest Meteorology* **151** (12), 1800–1811.

Shafer, B. A. & Dezman, L. E. 1982 Development of a surface water supply index (SWSI) to assess the severity of drought conditions in snow pack runoff areas. In: *Proceedings of the Western Snow Conference*. Colorado State University, Colorado, pp. 164–175.

Van Rooy, M. P. 1965 A rainfall anomaly index independent of time and space. *Notos* **14**, 43.

Vicente-Serrano, S. M. 2006 Differences in spatial patterns of drought on different time scales: an analysis of the Iberian Peninsula. *Water Resources Management* **20**, 37–60.

Vicente-Serrano, S. M. & López-Moreno, J. I. 2005 Hydrological response to different time scales of climatological drought: an evaluation of the standardized precipitation index in a mountainous Mediterranean basin. *Hydrology and Earth System Sciences* **9**, 523–533.

Vicente-Serrano, S. M., Begueria, S. & Lopez-Moreno, J. I. 2010 A multi-scalar drought index sensitive to global warming: the standardized precipitation evapotranspiration index-SPEI. *Journal of Climate* **23** (7), 1696–1718.

Wang, Y. X., Li, J. Z., Feng, P. & Chen, F. L. 2015a Effects of large-scale climate patterns and human activities on hydrological drought: a case study in the Luanhe River basin, China. *Natural Hazards* **76**, 1687–1710.

Wang, Y. X., Li, J. Z., Feng, P. & Hu, T. 2015b A time-dependent drought index for non-stationary precipitation series. *Water Resources Management* **15**, 1–17.

Wu, H., Hayes, M. J., Wilhite, D. A. & Svoboda, M. D. 2005 The effect of the length of record on the standardized precipitation index calculation. *International Journal of Climatology* **25**, 505–520.

Zarch, M. A. A., Sivakumar, B. & Sharma, A. 2015 Droughts in a warming climate: a global assessment of Standardized precipitation index (SPI) and Reconnaissance drought index (RDI). *Journal of Hydrology* **526**, 183–195.

Zargar, A., Sadiq, R., Naser, B. & Khan, F. I. 2011 A review of drought indices. *Environmental Reviews* **19**, 333–349.

First received 14 July 2015; accepted in revised form 24 October 2015. Available online 16 December 2015